

## Comparison of deep learning and regression-based MPPT algorithms in PV systems

Murat Salim KARABİNAOĞLU<sup>1,\*</sup>, Bekir ÇAKIR<sup>2</sup>

Mustafa Engin BAŞOĞLU<sup>3</sup>, Abdülvehhab KAZDALOĞLU<sup>4</sup>, Aziz GÜNEROĞLU<sup>5</sup>

<sup>1</sup>TÜBİTAK National Metrology Institute (TÜBİTAK UME), Kocaeli, Turkey

<sup>2</sup>Department of Electrical Engineering, Kocaeli University, Kocaeli, Turkey

<sup>3</sup>Department of Electrical and Electronics Engineering, Faculty of Engineering and Natural Sciences, Gümüşhane University

Received: 01.11.2021

Accepted/Published Online: 10.08.2022

Final Version: 28.09.2022

**Abstract:** Solar energy systems (SES) and photovoltaic (PV) modules should be operated at the maximum power point (MPP) to achieve the highest efficiency in the energy generation processes. Maximum power point tracking (MPPT) applications using conventional methods may not be able to follow the global MPP (GMPP) of the PV system under changing atmospheric conditions and they could oscillate around the local MPP. In this study, a machine learning and deep learning (DL) based long short-term memory (LSTM) model is proposed as an innovative solution for MPPT. Contrary to the traditional MPPT applications using current and voltage sensors, the output resistance of the PV module estimation was made by using environmental parameters (such as temperature and radiation) and artificial intelligence algorithms in this study. The LSTM model was compared with artificial neural networks (ANN) and regression methods regarding mean square error (MSE), root mean square error (RMSE) and mean absolute error (MAE) parameters. It has been determined that the LSTM model has a better performance and could more successfully follow MPP compared to the other methods. Finally, after the comparison with the ANN method, it is proved that LSTM gives 37%, 21%, and 31% more successful MSE, RMSE, and MAE results, respectively.

**Key words:** Maximum power point tracking, deep learning, long-short term memory, regression, artificial neural network

### 1. Introduction

Environmental negativities caused by energy generation methods using fossil fuels have made clean, sustainable and renewable energy generation systems much more important for the future of the world. Solar energy systems are one of the most preferred renewable energy sources today, as they are environmentally friendly and can be installed anywhere in the world with their increased efficiency.<sup>1</sup> MPPT algorithms and methods in the literature have generally provided solutions according to the dependence on PV module parameters, the ability to follow GMPP in partial shading conditions (PSCs), the need for analog or digital circuits, the need for periodic adjustment, the convergence speed of the MPP, the complexity level in the application and measured parameters [1–10]. Even though traditional methods are simple and easily applicable, they cannot follow the MPP and cause power losses in the long term. The most preferred traditional MPPT methods are perturbed and observed (P&O) and incremental conductance (IC) algorithms [11, 12]. Traditional P&O and

\*Correspondence: murat.karabinaoglu@tubitak.gov.tr

<sup>1</sup>IRENA(2021). International Renewable Energy Agency [online]. Website <https://www.irena.org/Statistics/View-Data-by-Topic/Capacity-and-Generation/Technologies> [accessed 05-04-2021].

IC methods with ANN models are used not only for comparison purposes but also as hybrid methods in many studies [5, 13–20]. PV modules can also be categorized into three as independent, grid-connected and hybrid according to their connection type to the grid [21]. The response performance of different MPPT methods under rapidly changing weather conditions were tested in a study with four different techniques as P&O, IC, hill climbing (HC), and fuzzy logic controller (FLC) [22]. According to the results obtained in the related study, it was determined that the FLC method had the best performance in the entire duty cycle range. On the other hand, various methods and solutions have been proposed for MPPT methods to follow GMPP under PSCs [5, 8–10, 23–31]. In a comprehensive study of 110 different research articles in the literature, thirty-one methods used for MPPT were examined in detail by considering thirteen parameters [32]. All examined MPPT methods are summarized with their advantages and disadvantages by considering thirteen parameters. As a result of the related study, it was stated that software computing techniques can produce very efficient results, but the complexity levels of these methods are high [32]. In another similar study, forty MPPT methods were examined in detail and all methods were modeled mathematically [1]. As an evolutionary technique, the "JayaDE" algorithm, which combines "Jaya" and "differential evolution (DE)" methods, was presented in a study on MPPT under rapidly changing atmospheric conditions [33]. According to the results obtained, the steady-state and dynamic performance of this mixed technique is superior to the state-of-the-art control methods in varying atmospheric conditions. In a PV system, fourteen different computational intelligence (CI) methods were compared in a study in which various CI techniques were examined under rapid irradiation changes and the PSC for MPPT [24]. In the related study, in which CI methods are divided into subcategories and examined in detail, the application of these methods in PV systems, their advantages and disadvantages are explained. In a study that presents a probability-based classification method as Bayesian for MPPT in PV systems, a controller was proposed for systems under changing irradiation and shading conditions [6]. In a study of mixed MPPT methods, twenty different combinations were examined in detail. Three of these methods is considered as simultaneous, nine as intelligent and eight as nonintelligent [7]. The result determined by the related study is that no single independent or mixed-method can give the optimum solution alone. This is because all methods have properties that vary according to convergence speed, efficiency, sensed parameters, application complexity and cost [7]. In a study examining AI-based methods, it was determined that seven basic AI-based MPPT techniques provide faster convergence, smaller steady-state oscillation and higher efficiency compared to traditional methods, while they are computationally intensive and costly applications [10]. In addition, it has been reported that swarm intelligence (SI), machine learning (ML) and DL methods are more preferable than FLC, ANN and genetic algorithm (GA) methods [10]. One of the novel methods that has come to the fore in recent years is the deep reinforcement learning (DRL) method for MPPT [34, 35]. It has been seen that the proposed DRL-based MPPT method can yield successful results due to its fast response and stable behavior. In an ML-based study, a new global MPPT method suitable for working in PSCs is presented [29]. The Q learning algorithm proposed in the related study was compared with the particle swarm optimization method. It has been observed that the presented algorithm reduces the time required to detect the global MPPT by 80.5%–98.3%. Table 1 summarizes some of the publications related to MPPT in 2021 in terms of contribution to the literature.

In this study, the LSTM method for MPPT was presented. The basic motivation for selecting LSTM is that it is an improved version of the recurrent neural network and it became a very popular method especially for time-series prediction and sequential behavior tracking problems recently which was explained below. In PV modules, GMPP has a nonlinear relationship with the parameters of irradiation, ambient temperature and

**Table 1.** Papers in 2021.

Year	Reference	Contribution
2021	[36]	This review is a detailed study of prediction applications in the field of solar energy based on machine learning. It is given as a compilation consisting of solar energy, radiation, power generation, electricity prices, energy demand estimation and extraction of design parameters in PV systems, efficiency and MGNI. It also provides an overview of many new and promising methods in PV systems.
2021	[37]	To increase the efficiency in PV systems, this study proposes the gray wolf optimization algorithm and radiation estimation and multicore extreme learning machine-based MPPT application. Simulations have shown that optimization and estimation studies give more successful results than traditional MPPT studies.
2021	[38]	It is presented in this paper that the developed MPPT-based regression controller can achieve the maximum peak voltage under different partial shading conditions. In this method, by estimating the booster type converter and duty ratio, it was stated that 20%, 16.96%, and 15% more efficient results were obtained from PSO, flower pollination algorithm, and P&O methods, respectively.
2021	[39]	This study proposes a general regression neural network method trained with a sailfish optimizer as a hybrid method. The proposed method was compared with the general regression neural network (GRSA)-sailfish optimiser and GRSA-P&O methods for rapid variation in radiation and partial shading conditions. The results obtained have proven that it follows the global MGN with 99.9% efficiency.
2021	[40]	This work is presented for MPPT using P&O, IC and fuzzy-PI methods and single-ended primary inductor converters with amplifier.
2021	[41]	This study presented a hybrid and two-stage MPPT method when sudden and rapidly changing environmental conditions occur. Segmentation-based MPPT and ANN-based MPPT methods and hill climbing method were used. The most important contribution of the study is that it shows that it can follow the GMPPT without any data on the environmental condition.
2021	[42]	This paper includes the comparison of the PSO algorithm according to different criteria for MPPT. As a result, it is presented that there are deterministic PSO methods in average efficiency and adaptive PSO methods incapturing the fastest MGN.
2021	[43]	In this study, the examination of hybrid, classical, smart and optimization-based techniques for MPPT is presented. The contribution of the study to the literature is that it is a compilation study to determine the most advantageous method in terms of certain applications for MPPT.
2021	[44]	This study proposes a backstepping terminal sliding mode control (BTSMC) algorithm for MPPT. The proposed method is compared with P&O, PID and backstepping nonlinear MGNI controller. As a result, it has been proven that the proposed method performs better under rapidly changing conditions in terms of monitoring and convergence criteria.

PSCs that change continuously during the day. Being able to follow the GMPP accurately and quickly will make the MPPT method more successful. In order to find a solution for this problem, the LSTM method has been proposed. The proposed LSTM model was compared with ANN and linear regression methods considering the PV panel's MPPT performances. All analyzes were made by using Python 3.7 software and implemented in the form of simulation. The data of a PV system integrated into a three-phase grid with a power of 3.62kW, which is under the responsibility of the Kocaeli University Faculty of Engineering has been used. The performances of LSTM and all the others were compared by using atmospheric measurement parameters of 2018 such as irradiation, ambient temperature and humidity data. It has been found that the LSTM model produces better results. In this study, it is assumed that the DC-DC converter which converts the PV module output voltage to the level required by the load is used for MPPT in PV modules. How accurately the MPP can be predicted and followed was examined by using ANN, LSTM, and linear regression methods. The contributions of this article are summarized as follows:

- The resistance of the PV module was predicted by LSTM, ANN and regression-based models for MPPT applications.
- One of the best novelties for this study is there was not used any voltage, current or power sensor while predicting the output power of the PV module except for the training phase.
- It was proved that LSTM has 37%, 21%, and 31% percent more successful prediction results than ANN regarding MSE, RMSE, and MAE parameters, respectively.
- This was a promising work that shows that AI or ML-based methods can be used together with traditional methods or to perform MPPT studies with different AI algorithms in the future.
- This was also a challenging work for sensorless MPPT applications. It also needs to be improved by optimizing models more and included some other novel algorithms in it.

This paper is organized as follows: In Section 2, the basic information about the MPPT process and the basic equations of the PV module are given and the applied MPPT methods are presented. In addition, the basic relations are given according to the steady-state analysis of the boost DC-DC converter. In Section 3, information about the PV panel and data collection system is given. ML and regression-based MPPT methods are examined in the fourth part of the study. Evaluations regarding the analysis carried out are given in the fifth section and finally the results and prospective section are presented.

## 2. MPPT

PV modules are DC power supplies that produce current and voltage according to the environmental conditions and the impedance value of the load connected at the output. PV modules consist of a series connections of solar cells with a voltage of 0.5–0.6V. The current-voltage (I-V) and power-voltage (P-V) curves of a typical solar cell have given in Figure 1. MPPT process should be performed to continuously take maximum power from the PV modules for changing environmental conditions and load situations. The solar cell current equation is written as follows when a single diode solar cell is referenced.

$$I_{PV} = I_{SC} - I_{RS} \left[ \exp \left( \frac{V_{PV} + R_S I_{PV}}{V_T} \right) - 1 \right] - \frac{V_{PV} + I_{PV} R_S}{R_P} \quad (1)$$

In the single diode equivalent circuit in Equation (1),  $I_{PV}$  is the PV module current,  $I_{SC}$  is the short circuit current,  $I_{RS}$  is the diode reverse saturation current,  $V_{pv}$  is the PV module current,  $V_T$  is the thermal voltage,  $I_{RS}$  is series contact resistance and  $R_P$  is parallel resistance. The PV module can only give a maximum power at one point as shown in Figure 1. The operating voltage and operating current are shown which correspond to the MPP under a certain temperature and irradiation. The MPP of a PV module varies depending on the irradiation intensity, module and ambient temperature and shading conditions. The effects of different irradiance values on the MPP under constant temperature are shown in Figure 2 as I-V and P-V curves of the module. The short-circuit current of the PV module ( $I_{SC}$ ) changes in direct proportion to the insolation and is a function of the insolation.

$$I_{SC} = I_{SC,STC} \frac{Q_A}{Q_R} - K_I(T_A - T_R) \tag{2}$$

$I_{SC,STC}$  in Equation (2) is the short-circuit current under standard test conditions,  $Q_A$  is the instantaneous irradiation,  $Q_R$  is the reference irradiation,  $K_I$  is the temperature-dependent current coefficient of variation,  $T_A$  is the instantaneous temperature,  $T_R$  is the reference temperature.

The ambient temperature where the PV module located is another important parameter on the performance and efficiency of the PV module. I-V and P-V curves of the panel are given in Figure 3 for constant irradiation and different operating temperatures. As shown in Figure 3, depending on the increasing of the temperature, the short circuit current increases proportionally whereas the open-circuit voltage decreases logarithmically.

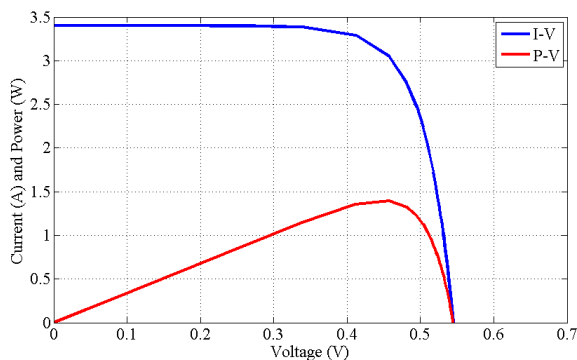


Figure 1. I-V and P-V curves of a typical solar cell.

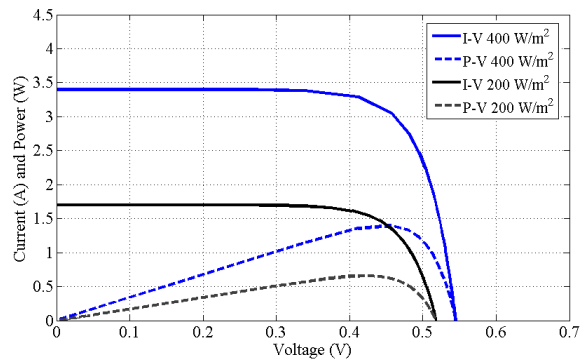


Figure 2. I-V and P-V characteristics for constant temperature and different irradiance.

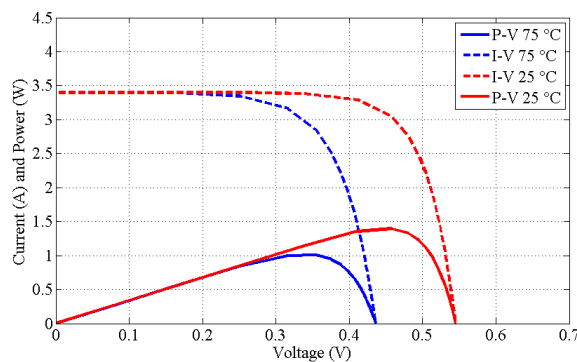


Figure 3. I-V and P-V characteristics of the PV module under constant irradiation and different operating temperatures.

### 2.1. MPPT algorithms

Many MPPT algorithms and methods have been proposed in the literature. These algorithms can be categorized based on criteria such as complexity level, sensor requirements, speed of convergence, cost, range of effectiveness, application hardware, and popularity. These algorithms and methods can be categorized into four groups: traditional methods (P-O, IC and HC), artificial intelligence (AI)-based approaches (ANN, fuzzy logic, etc.), indirect methods (curve fitting and look-up table, etc.) and hybrid methods.

### 2.2. Partial shading conditions (PSCs)

In recent years, it has been determined that partial shading has significant effects on the P-V characteristic curves, apart from irradiation and module temperature. The partial shading situation is shown with the example of two modules given in Figure 4. Increasing the performance of the PV system, deactivating the low-irradiation module in case of shading and eliminating the hot-spot problem that may occur are provided by the use of bridge diodes.

Figure 4 shows a system with two PV modules and one of them receives 1000 W/m<sup>2</sup> and the other 400 W/m<sup>2</sup> irradiation. Since the amount of irradiation falling on the surfaces of the two PV modules is different, the current and voltage produced by these two modules will be different. The P-V and I-V characteristic curves of the system under PSC are shown in Figure 5.

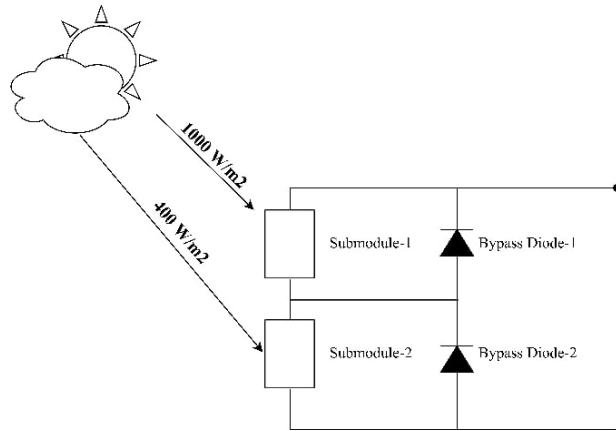


Figure 4. PV module state under partial shading.

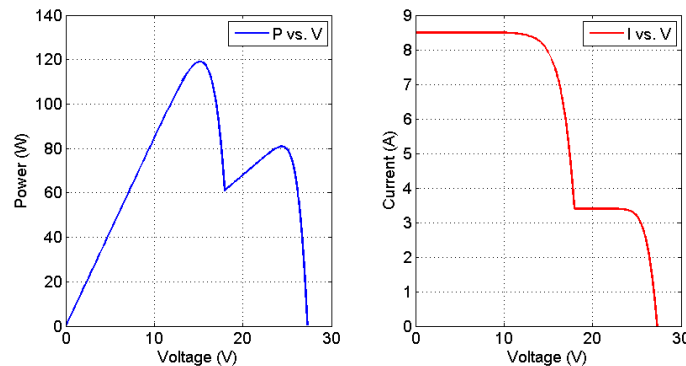


Figure 5. P-V and I-V curves under PSCs.

In summary, the MPP of PV modules is highly dependent on changing environmental conditions. The main purpose with MPPT is to bring the operating point that differs depending on the environmental changes to the point where the PV module provides maximum power. It is critical not to stay in the local MPP especially under PSCs and to be able to follow the GMPP under all conditions. For this reason, various MPPT methods will be tested under varying atmospheric conditions so that they can adapt to irradiation or shading conditions as quickly as possible.

### 2.3. Boost DC-DC converter

Boost DC-DC converters are used in PV systems to increase the output voltages of the PV modules to the voltage level required by the load. The ideal schematic of a boost type DC-DC converter is shown in Figure 6.

A typical boost DC-DC converter consists of an inductance, a switch, a diode and a capacitor. The switch represented as T is controlled by using pulse width modulation (PWM). When the switch is closed, the current passing through the inductance increases and energy is stored in the inductance. The power required for the load is provided via capacitor C. When the T switch is opened, the current flowing from the PV module panel is used to charge the output capacitor through the inductance and diode and feed the load at the same time. The waveforms of a typical boost type DC-DC converter are shown in Figure 7, where all elements are considered ideal, the load is pure ohmic, and the switching time is much shorter than the electrical time constant of the circuit.

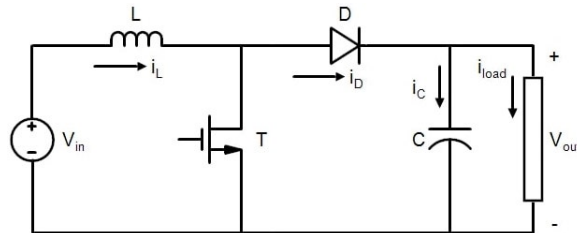


Figure 6. Boost DC-DC converter.

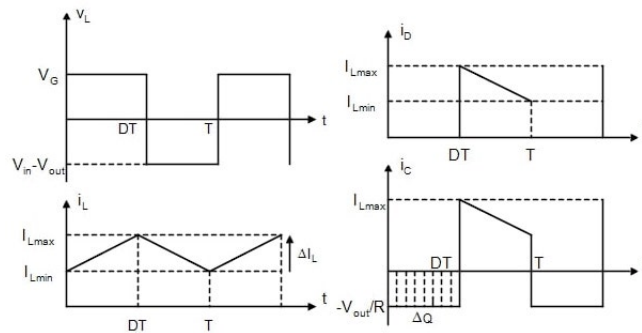


Figure 7. Boost DC-DC converter waveforms.

In steady-state operation of the converter, the average coil voltage is zero for the entire switching period. Under these conditions, the converter output voltage is obtained using Equation (3).  $V_{out}$  is the output voltage,  $V_{in}$  is the input voltage,  $D$  is the duty cycle in Equation (3).

$$V_{out} = \frac{V_{in}}{1 - D} \quad (3)$$

The analysis were carried out using the data of the thin-film PV module made of Cd-Te material. Detailed features of the system used in this study are given in Table 2. A sample data set from the data captured through the web interface of the system<sup>2</sup> is given in Table 3. The measured parameters are averaged in five-minute periods and stored in the database. The recorded data includes the temperature, irradiation, power and voltage of the PV system for almost a year.  $R_{PV}$  is the panel output resistance and was calculated according to Equation (4) from the power and voltage data in Table 3.

$$R_{PV} = \frac{V^2}{P} \quad (4)$$

**Table 2.** Feature of installed PV modules and sensor box [45].

	Module technology			Sensor box	
	c-Si	mc-Si	Cd-Te	Solar irradiation sensor	
Maximum power current (A)	8.3	8.35	3.7	PV cell type	a-Si
Maximum power voltage (V)	138.8	149.7	163	Measurement range	0-1500 W/m <sup>2</sup>
Maximum power (W)	1170	1250	1200	Accuracy	±8%
Number of PV modules	6	5	8	Resolution	1W/m <sup>2</sup>
Connection	6S	5S	4S2P	Temperature sensor	
Area (m <sup>2</sup> )	7968	8315	9824	Measuring sensor	PT100
Inverter	SMA 1300 TL (1300Wp)			Measurement range	-20 °C to 110 °C
Inverter measurement accuracy	DC: ± 4% , AC: ± 3%			Accuracy	± 0.5%
Web box	For monitoring by internet			Resolution	0.1 C°

**Table 3.** Sample data set.

Temperature (°C)	Irradiation (W/m <sup>2</sup> )	Power (W)	Voltage (V)	$R_{PV}$ (Ω)
6.97	293.23	460.65	348.69	263.94
7.88	311.11	438.68	342.75	267.80
11.15	445.72	617.82	345.02	192.68
12.49	519.86	684.78	343.50	172.31
14.73	583.53	742.27	341.30	156.93
15.92	637.84	792.81	339.49	145.37
17.35	682.91	833.85	337.47	136.58
18.02	724.17	870.23	337.24	130.69
19.10	755.13	895.54	335.77	125.89
19.93	782.89	919.05	334.79	121.96
19.04	821.00	955.33	334.89	117.40
18.99	843.27	974.67	334.66	114.91
18.69	855.62	986.80	335.37	113.98
19.92	857.38	985.02	334.80	113.80
20.78	856.77	980.60	333.54	113.45
20.85	857.52	979.98	333.03	113.17
21.86	852.81	975.24	332.91	113.64
22.23	829.20	949.19	332.54	116.50
22.30	795.45	914.56	333.19	121.39

<sup>2</sup>SMA(2021). SMA Solar Technology AG - Sunny Portal [online]. Website <https://www.sunnyportal.com> [accessed 05-04-2021].



Figure 8 depicts the MPPT scheme in this paper.  $I_{PV}$  and  $V_{PV}$  represent the voltage and current of the panel, respectively, in Figure 8.  $R_{load}$  is the load resistance,  $V_{out}$  and  $I_{out}$  represent the voltage and current at the DC-DC converter output.

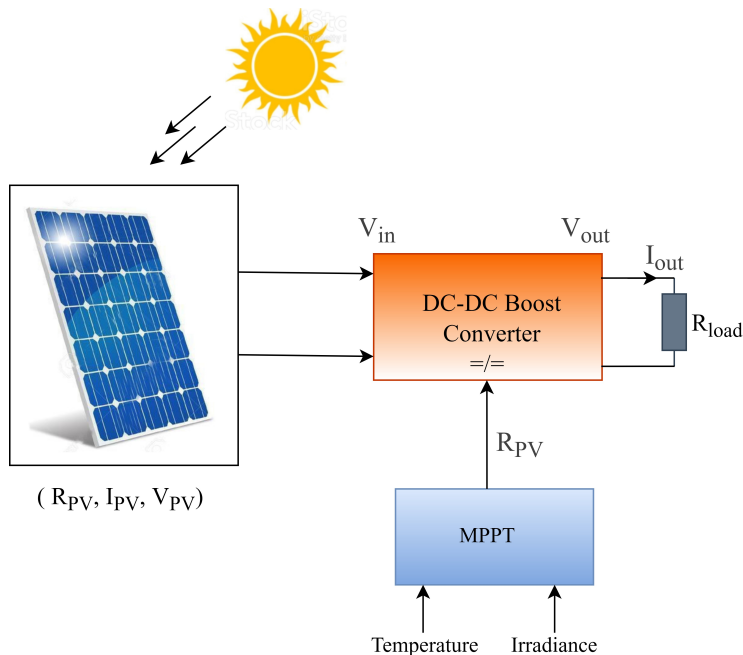


Figure 8. MPPT scheme.

$R_{load}$  is assumed constant as  $1200\Omega$  in this study. The DC-DC converter duty cycle ( $D$ ) is calculated by Equation (5).

$$D = 1 - \sqrt{\frac{R_{PV}}{R_{load}}} \tag{5}$$

The DC-DC converter output voltage ( $V_{out}$ ) is calculated by Equation (3). The power to be transferred to the load at the DC-DC converter output is calculated by Equation (6).

$$P = \frac{V_{out}^2}{R_{load}} \tag{6}$$

### 3. Machine learning and regression-based MPPT techniques

ANN is the most widely used form of DL which is a subset of ML. The first version of neural networks consisted of simple neural layers for perceptron[46]. In the second version, the backpropagation algorithm is used to update it according to the weights and error rates between neurons. The Bounded Boltzmann Machine, which facilitates learning, is proposed to deal with the limitations of backpropagation. Then, feed-forward neural networks (FNN), convolutional neural networks (CNN), recurrent neural networks (RNN), etc. which are other methods and neural networks were introduced.

### 3.1. Artificial neural networks (ANN)

#### 3.1.1. Methodology

ANN method is evaluated within indirect and AI methods and it is generally created using three layers (input-hidden-output). In this study, the input layer parameters of ANN are PV module voltage, PV module current and atmospheric conditions such as temperature and solar irradiation level. In the output layer of the ANN, voltage, current or the output resistance of the PV module parameters are produced as a reference signal. By this way, it is ensured that the system operates on a point close to the MPP.

Since the I-V and P-V relationships of the PV module are nonlinear, the neural network estimates the output resistance of the PV module by using the input parameters temperature and irradiation. The proposed ANN model consists of a multilayer perceptron, an input layer with two neurons, a hidden layer with 32 neurons, and an output layer with a neuron as shown in Figure 9. A total of 96 weight parameters between the three layers converge towards the new values suitable for the desired model at the end of the training process, according to the values given at the beginning.

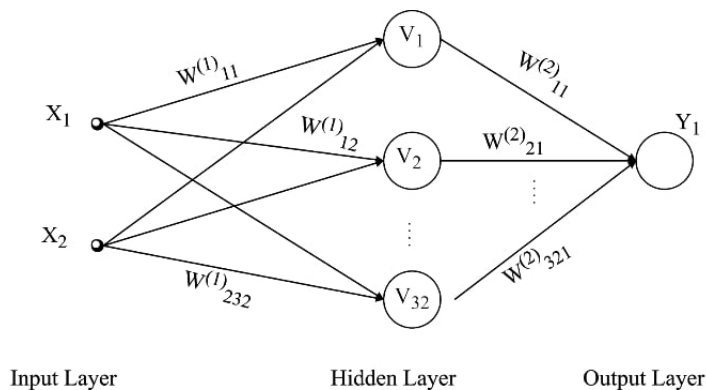


**Figure 9.** ANN model.

The advantage of the ANN method is that it can reveal the nonlinear correlation between certain input parameters and the desired output parameter. On the other hand, the disadvantages of ANN are that it depends on the characteristics of the panel and it is necessary to repeat the training process of the network as atmospheric conditions change. In the last decade, AI techniques have been widely used for MPPT in solar energy systems. This is because conventional MPPT techniques cannot follow GMPP under the PSC. The P-V output curve for a PV module has only one GMPP and correspondingly at least one LMPP. The application of AI for the purpose of MPPT is very important to keep track of the GMPP while increasing the overall efficiency and performance of the MPPT. The selection of AI-based MPPT techniques is complex because each technique has its own merits and demerits.

The integration of various AI optimization techniques with MPPT aims to complete the following shortcomings of traditional methods:

- Lack of adaptive, robust and self-learning abilities.
- Power swing and slow, steady-state responses in MGN with high steady-state error.
- Unable to find GMPP, stay in LMPP and incorrect mixing direction under partial shading.

In general, all AI-based MPPT techniques provide fast convergence, less steady-state oscillations, and higher efficiency compared with conventional MPPT techniques. However, AI-based MPPT techniques are computationally intensive due to training, validation and testing processes and are costly due to the hardware requirements to perform these calculations.

### 3.1.2. Results

Figure 10 depicts the actual and predicted panel output resistance ( $R_{pv}$ ) by using ANN model. The calculation of the  $R_{pv}$  was explained before with Equation (4).

The  $R_{pv}$  was found as the target output thanks to the temperature and radiation data of the environment where the PV module is located before the training process. The results show that the ANN model could track  $R_{pv}$  successfully even though there was no current and voltage sensor during estimation in Figure 10. The mean absolute error of the  $R_{pv}$  is about  $137\Omega$ .

Besides, the output power estimation using the ANN model is shown in Figure 11. Power calculation has been explained previously with Equation (6) by using DC-DC converter output voltage and load resistance. The results show that the mean absolute error of the output power is about 211 W for about 900 data points at the test process. While considering the maximum output power which corresponds to 1200 W for PV module system MAE value is about 17.6%.

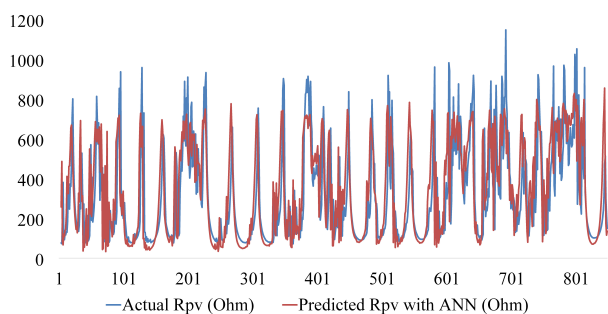


Figure 10.  $R_{pv}$  by ANN.

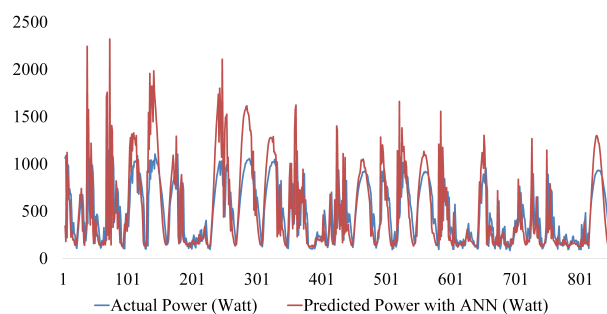


Figure 11. Output power by ANN.

## 3.2. Regression method

### 3.2.1. Methodology

Regression analyses are one of the most widely used methods to determine the relationship between two variables in statistical solutions. Regression analysis can be categorized as linear and nonlinear regression analysis according to the distribution of data. The regression model with the best ability to follow the GMPP was desired to be produced by this study. For this reason, temperature and irradiation parameters were used as the independent variables and the output resistance of the PV module was used as the dependent variable and curve fitting was performed. About 75% of all samples in the dataset were used to find the variables in the regression equation and the remaining 25% were used for testing.

In its simplest definition, linear regression is the type of curve that will form a straight line in bivariate (x, y) form. The relation formed as a result of curve fitting using temperature and irradiation values for the application of the MPPT algorithm is given in Equation (7).

$$y = \beta_0 + \beta_1 * X_1 + \beta_2 * X_2 + u \quad (7)$$

Here,  $y$  represents the output resistance of the PV module as the dependent variable, and  $X_1$  and  $X_2$  represent the independent variables that make up the irradiation and temperature.  $\beta_0$ ,  $\beta_1$  and  $\beta_2$  are constant regression coefficients. The term  $u$  is expressed as the amount of error.

### 3.2.2. Results

Figures 12 and 13 show the graph of the output resistance of the PV module and output power which are trying to be estimated using the linear regression method.

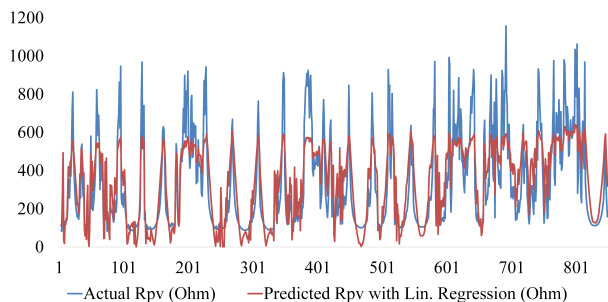


**Figure 12.**  $R_{pv}$  by linear regression.

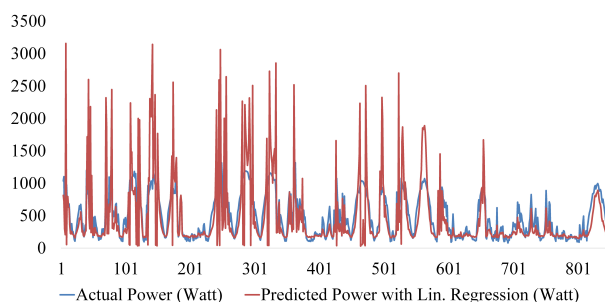


**Figure 13.** Output power by linear regression.

The results show that the linear regression model could predict  $R_{pv}$  and output power with the mean absolute error value of  $566,6\Omega$  and  $223,1W$  respectively.

Our main purpose in this article is to prove that MPPT can be applied with only ambient conditions parameters without reading any electrical parameters such as current, voltage or power from PV panels instantly. It was observed that the ANN and regression models could not be as successful as LSTM in modeling the data set due to the nonlinear characteristic of the PV data. For this reason, there could be high estimation differences in some regions between the actual and predicted data points in Figures 11–Figure 13.

## 3.3. Deep learning - LSTM

### 3.3.1. Methodology

The term DL was first introduced in the field of machine learning in 1986 and it was used for ANN in 2000 [47]. The concept of DL allows computers to learn more complex structures from smaller parts [48]. DL methods consist of multiple layers to learn the properties of data with multiple levels of abstraction [49]. DL is a structure that uses algorithms inspired by the structure and function of the brain called ANN. It is also a subset of ML capable of supervised or unsupervised learning, classification and pattern recognition. RNNs are sequence-based models in which the output is not only dependent on the current input parameter, but can also be created depending on other input variables unlike traditional feed-forward neural networks. In RNNs, the output layers form the input to the next network. RNN structures can be used especially for time series prediction and sequential behavior tracking problems. Since the decision made at time  $t-1$  affects the decision to be made at time  $t$ , RNNs are preferred to solve these problems. In RNNs, the input data is applied as a series and the outputs are found again considering the previous results. With this feature, RNN structures have the ability to hold information like memory [50]. Figure 14 shows a simple RNN model and a cascaded form of this model.

A standard RNN has a layer that uses hyperbolic tangent ( $\tanh$ ) as the activation function. In RNNs, training is done by backpropagation [51]. LSTM networks are a type of RNN architecture and it was brought

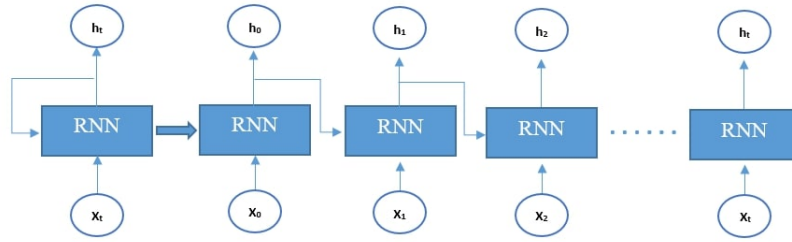


Figure 14. RNN model.

to the literature by Hochreiter and Schmidhuber [52]. Later, it was developed by Gers by adding the forget gate and has become very popular today [53]. The general structure of LSTM has been studied in detail by Lipton et al. [54]. LSTM networks were developed to avoid the long-term dependency and vanishing-exploding gradient problems in RNNs. Figure 15 shows a basic LSTM structure.

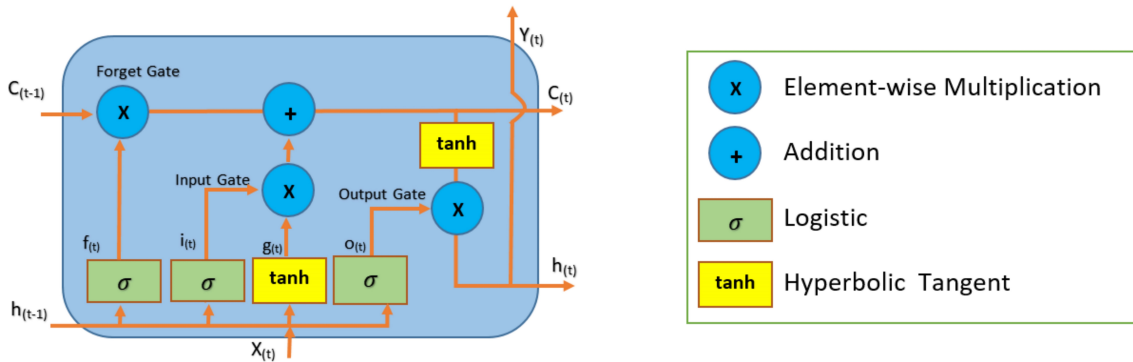


Figure 15. LSTM general structure.

The forget gate seen in Figure 15 determines which part of the cell state information should be forgotten according to the current input values and the output values at the previous moment and is expressed with the following equation.

$$f_t = \sigma(W_f X_t + U_f h_{t-1} + b_f) \tag{8}$$

In Equation 8,  $W_f$  and  $U_f$  are weight matrices.  $b_f$  is bias vectors.  $X_t$  shows the current input.  $h_{t-1}$  is the output at time t-1. The input gate consists of 2 layers as sigmoid and tanh. The sigmoid layer is used to control which information of the tanh layer is added to the current cell state in Equation 9. The tanh layer is used to generate a new candidate vector in Equation 10.

$$i_t = \sigma(W_i X_t + U_i h_{t-1} + b_i) \tag{9}$$

$$\tilde{C} = \tanh(W_i X_t + U_i h_{t-1} + b_i) \tag{10}$$

The output gate is the part that determines the information flowing to the rest of the network in Equations 11–13.

$$o_t = \sigma(W_o X_t + U_o h_{t-1} + b_o) \tag{11}$$

$$C_t = i_t * \tilde{C}_t + f_t * C_{t-1} \tag{12}$$

$$h_t = o_t * \tanh(C_t) \quad (13)$$

In Equations 11–13  $W_i, U_i, W_z, U_z, W_0$  and  $U_0$  are weight matrices.  $b_t, b_z$  and  $b_0$  are bias vectors.  $h_t$  is the outputs at time t. Sigmoid and hyperbolic tangent functions are expressed in Equations 14 and 15.

$$\sigma(x) = \frac{1}{1 + e^{-x}} \quad (14)$$

$$\tanh(x) = \frac{e^x - e^{-x}}{e^x + e^{-x}} \quad (15)$$

Prediction-based studies using LSTM have become very popular, especially in recent years with DL applications [55–57]. For example, LSTM network can produce predictions with lower RMS errors than the more traditional ARMA model, ARFIMA model and BPNN models [58]. It is stated that the CNN-LSTM network has better performance with an MSE of 0.37 compared with the conventional estimation methods for the dataset of individual household power consumption [55]. Moreover, it has been proved that the LSTM method could make predictions with a smaller error compared to MLR (multiple linear regression), BRT (bagged regression trees) and NN (neural networks) methods [59].

### 3.3.2. Results

The structure of the LSTM model used in this study is shown in Figure 16. The structure consists of five layers. The first and second LSTM layers have 10 and 30 hidden layers, respectively.

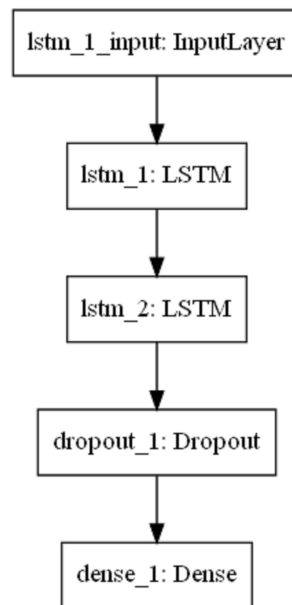


Figure 16. LSTM flow chart.

The weight updates in the LSTM model were added randomly to prevent overfitting in the dropout layer of our model. The estimated result of the output resistance of the PV module was obtained at the output of the dense layer. As a result, 5511 trainable parameters are used in the entire model.

Figure 17 depicts the actual and predicted Rpv by using LSTM model. The Rpv is the output feature of the LSTM while the input features are also the temperature and radiation data of the environment. The results show that the LSTM model could follow Rpv with the mean absolute error value of 95.2 Ω.

Besides, the output power estimation using the LSTM model is shown in Figure 18. The results show that the mean absolute error of the output power is about 143 W for about 900 data points at the test process. While considering the maximum output power which corresponds to 1200 W for PV module system MAE value is about 11.9%.

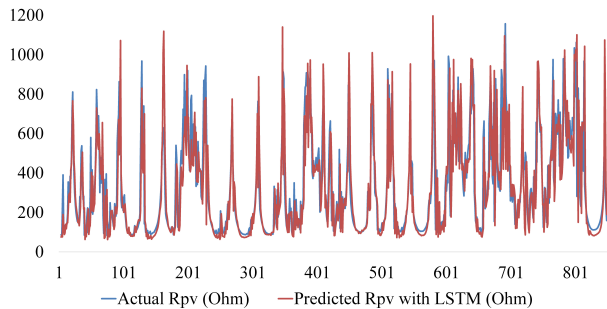


Figure 17.  $R_{pv}$  by LSTM.

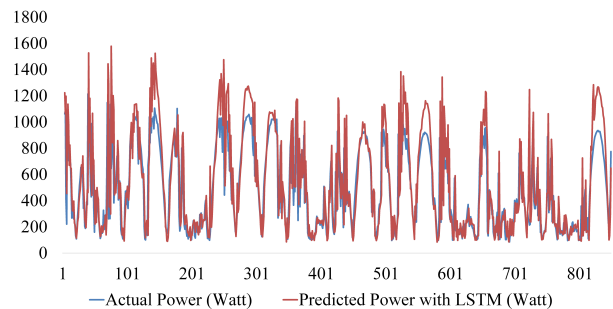


Figure 18. Output power by LSTM.

#### 4. Discussion

In this paper, the comparison of DL and regression-based MPPT algorithms is discussed. Figure 19 depicts the sample dataset which includes temperature, irradiation and Rpv of the system which are mentioned in detail before. Each feature has 3580 data points separately. The second axis of the graph represents the temperature parameter of the system. In addition, 2600 pieces of data, which corresponds to approximately 75% of the entire data set, were used for training and validation procedures. The remaining 25% of the data set was used for testing.

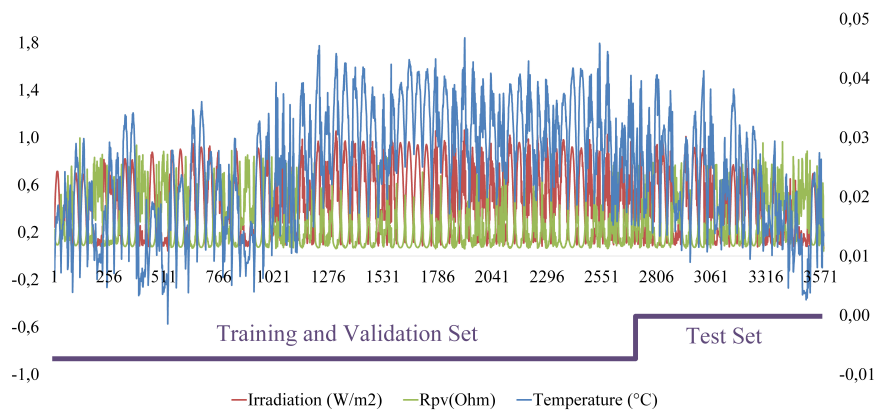


Figure 19. Sample dataset.

The comparison was performed using LR, ANN and LSTM methods. The predicted power results are obtained leveraging these methods. To be able to determine which method follows the power more successfully, the prediction methods were compared by using MSE, RMSE, and MAE statistical metrics. The equations of

these metrics are explained in Equations 16–18.

$$MSE = \frac{1}{N} \sum_{i=1}^N (P_{actual} - P_{predicted})^2 \quad (16)$$

$$RMSE = \sqrt{\frac{1}{N} \sum_{i=1}^N (P_{actual} - P_{predicted})^2} \quad (17)$$

$$MAE = \frac{1}{N} \sum_{i=1}^N |P_{actual} - P_{predicted}| \quad (18)$$

In Equations 16–18,  $N$  is the total test sample count,  $P_{actual}$  and  $P_{predicted}$  are the actual and predicted power, respectively. The prediction methods were compared with MSE, RMSE, and MAE parameters as criteria. The normalized comparison results are shown in Table 4.

**Table 4.** Performance comparison of applied methods.

Method	MSE	RMSE	MAE
Linear regression	0.3226	0.5979	0.4721
ANN	0.0254	0.1593	0.1142
LSTM	0.0159	0.1261	0.0793

As a result of the comparison made between the applied methods, the LSTM model gave the best estimation performance with an RMSE value of 0.1261 and the linear regression model which has the worst estimation performance with an RMSE value of 0.5979.

## 5. Conclusion

The number of DL-based approaches is quite few for MPPT. Especially the success of these methods in forecasting problems in different fields has led to the formation of the MPPT method with an LSTM-based approach. In this study, the application of the LSTM method which is a model of recurrent neural networks for variable atmospheric conditions for MPPT in PV modules is presented. The advantage of the method proposed in this study is that it can predict the output resistance of the PV module during MPPT without the need for extra current and voltage sensors. On the other hand, the performance of a method such as LSTM, which has become popular in recent years on MPPT and its comparison with other methods has come to the fore in this study. The performance of the proposed LSTM model is compared with ANN, and LR methods. Irradiation and temperature data of 2018 are used at the input of four different models and the output resistance of the PV module is estimated at the outputs. When the LSTM model which gives the best results among the applied methods is compared with the ANN method regarding MSE, RMSE, and MAE parameters, it is proved that the LSTM model gives 37%, 21%, and 31% more successful results, respectively. In future studies, it is planned to apply hybrid methods where AI and ML-based methods can be used together with traditional methods or to perform MPPT studies with different AI algorithms.



## References

- [1] Karami N, Moubayed N, Outbib R. General review and classification of different MPPT Techniques. *Renewable and Sustainable Energy Reviews* 2017; 68: 1-8. doi: 10.1016/j.rser.2016.09.132
- [2] Esumi T, Chapman PL. Comparison of photovoltaic array maximum power point tracking techniques. *IEEE Transactions on Energy Conversion* 2007; 22 (2): 439-449. doi: 10.1109/TEC.2006.874230
- [3] De Brito MA, Galotto L, Sampaio LP, e Melo GD, Canesin CA. Evaluation of the main MPPT techniques for photovoltaic applications. *IEEE Transactions on Industrial Electronics* 2012; 60 (3): 1156-1167. doi: 10.1109/TIE.2012.2198036
- [4] Reisi AR, Moradi MH, Jamasb S. Classification and comparison of maximum power point tracking techniques for photovoltaic system: A review. *Renewable and Sustainable Energy Reviews* 2013; 19: 433-443. doi: 10.1016/j.rser.2012.11.052
- [5] Ram JP, Babu TS, Rajasekar N. A comprehensive review on solar PV maximum power point tracking techniques. *Renewable and Sustainable Energy Reviews* 2017; 67: 826-847. doi: 10.1016/j.rser.2016.09.076
- [6] Keyrouz F. Enhanced Bayesian based MPPT controller for PV systems. *IEEE Power and Energy Technology Systems Journal* 2018; 5 (1): 11-17. doi: 10.1109/JPETS.2018.2811708
- [7] Batarseh MG, Za'ter ME. Hybrid maximum power point tracking techniques: A comparative survey, suggested classification and uninvestigated combinations. *Solar Energy* 2018; 169: 535-555. doi: 10.1016/j.solener.2018.04.045
- [8] Bingöl O, Özkaya B. A comprehensive overview of soft computing based MPPT techniques for partial shading conditions in PV systems. *Mühendislik Bilimleri ve Tasarım Dergisi* 2019; 7 (4): 926-939. doi: 10.21923/jesd.570887
- [9] Yang B, Zhong L, Zhang X, Shu H, Yu T et al. Novel bio-inspired memetic salp swarm algorithm and application to MPPT for PV systems considering partial shading condition. *Journal of Cleaner Production* 2019; 215: 1203-1222. doi: 10.1016/j.jclepro.2019.01.150
- [10] Yap KY, Sarimuthu CR, Lim JM. Artificial intelligence based MPPT techniques for solar power system: A review. *Journal of Modern Power Systems and Clean Energy* 2020; 8 (6): 1043-1059. doi: 10.35833/MPCE.2020.000159
- [11] Femia N, Petrone G, Spagnuolo G, Vitelli M. Optimization of perturb and observe maximum power point tracking method. *IEEE Transactions on Power Electronics* 2005; 20 (4): 963-973. doi: 10.1109/TPEL.2005.850975
- [12] Likhith K, Tejas TN, Charan KY, Hosamane V, Bharati SK. Design and Development of an Efficient Photovoltaic System with Maximum Power Point Tracking Technique. *International Journal of Engineering Research & Technology (IJERT) NCESC* 2018; 6 (13).
- [13] Amrouche B, Belhamel M, Guessoum A. Artificial intelligence based P&O MPPT method for photovoltaic systems. *Revue des Energies Renouvelables ICRESD-07 Tlemcen* 2007: 11-6.
- [14] Rizzo SA, Scelba G. ANN based MPPT method for rapidly variable shading conditions. *Applied Energy* 2015; 145: 124-132. doi: 10.1016/j.apenergy.2015.01.077
- [15] Sindhura LS, Chaudary K. Artificial neural network implementation for maximum power point tracking of optimized solar panel. *International Journal of Computer Applications* 2013; 78 (10).
- [16] Khanaki R, Radzi MA, Marhaban MH. Comparison of ANN and P&O MPPT methods for PV applications under changing solar irradiation. In: 2013 IEEE Conference on Clean Energy and Technology (CEAT); Lankgawi, Malaysia; 2013. pp. 287-292.
- [17] Bouselham L, Hajji M, Hajji B, Bouali H. A new MPPT-based ANN for photovoltaic system under partial shading conditions. *Energy Procedia* 2017; 111: 924-933. doi: 10.1016/j.egypro.2017.03.255
- [18] Chtouki I, Wira P, Zazi M. Comparison of several neural network perturb and observe MPPT methods for photovoltaic applications. In: 2018 IEEE International Conference on Industrial Technology (ICIT); Lyon, France; 2018. pp. 909-914.

- [19] Çelikel R, Gündoğdu A. ANN-Based MPPT Algorithm for Photovoltaic Systems. *Turkish Journal of Science and Technology*. 2020; 15 (2): 101-110.
- [20] Saravanan S, Babu NR. Maximum power point tracking algorithms for photovoltaic system—A review. *Renewable and Sustainable Energy Reviews* 2016; 57: 192-204. doi: 10.1016/j.rser.2015.12.105
- [21] Salas V, Olias E, Barrado A, Lazaro A. Review of the maximum power point tracking algorithms for stand-alone photovoltaic systems. *Solar Energy Materials and Solar Cells* 2006; 90 (11): 1555-1578. doi: 10.1016/j.solmat.2005.10.023
- [22] Rezk H, Eltamaly AM. A comprehensive comparison of different MPPT techniques for photovoltaic systems. *Solar Energy* 2015; 112: 1-1. doi: 10.1016/j.solener.2014.11.010
- [23] Patel H, Agarwal V. Maximum power point tracking scheme for PV systems operating under partially shaded conditions. *IEEE Transactions on Industrial Electronics* 2008; 55 (4): 1689-1698. doi: 10.1109/TIE.2008.917118
- [24] Oulcaïd M, El Fadil H, Yahya A, Giri F. Maximum power point tracking algorithm for photovoltaic systems under partial shaded conditions. *IFAC-PapersOnLine* 2016; 49 (13): 217-222. doi: 10.1016/j.ifacol.2016.07.954
- [25] Jiang LL, Srivatsan R, Maskell DL. Computational intelligence techniques for maximum power point tracking in PV systems: A review. *Renewable and Sustainable Energy Reviews* 2018; 85: 14-45. doi: 10.1016/j.rser.2018.01.006
- [26] Alabedin AZ, El-Saadany EF, Salama MM. Maximum power point tracking for photovoltaic systems using fuzzy logic and artificial neural networks. In: 2011 IEEE Power and Energy Society General Meeting; Detroit, MI, USA; 2011. pp. 1-9. doi: 10.1109/PES.2011.6039690
- [27] Behera MK, Saikia LC. A new combined extreme learning machine variable steepest gradient ascent MPPT for PV system based on optimized PI-FOI cascade controller under uniform and partial shading conditions. *Sustainable Energy Technologies and Assessments* 2020; 42: 100859. doi: 10.1016/j.seta.2020.100859
- [28] Eltamaly AM, Farh HM. Dynamic global maximum power point tracking of the PV systems under variant partial shading using hybrid GWO-FLC. *Solar Energy* 2019; 177: 306-316. doi: 10.1016/j.solener.2018.11.028
- [29] Mao M, Cui L, Zhang Q, Guo K, Zhou L, Huang H. Classification and summarization of solar photovoltaic MPPT techniques: A review based on traditional and intelligent control strategies. *Energy Reports* 2020; 6: 1312-1327. doi: 10.1016/j.egyr.2020.05.013
- [30] Kalogerakis C, Koutroulis E, Lagoudakis MG. Global MPPT based on machine-learning for PV arrays operating under partial shading conditions. *Applied Sciences* 2020; 10 (2): 700. doi: 10.3390/app10020700
- [31] Fares D, Fathi M, Shams I, Mekhilef S. A novel global MPPT technique based on squirrel search algorithm for PV module under partial shading conditions. *Energy Conversion and Management* 2021; 230: 113773. doi: 10.1016/j.enconman.2020.113773
- [32] Verma D, Nema S, Shandilya AM, Dash SK. Maximum power point tracking (MPPT) techniques: Recapitulation in solar photovoltaic systems. *Renewable and Sustainable Energy Reviews* 2016; 54: 1018-1034. doi: 10.1016/j.rser.2015.10.068
- [33] Kumar N, Hussain I, Singh B, Panigrahi BK. Rapid MPPT for uniformly and partial shaded PV system by using JayaDE algorithm in highly fluctuating atmospheric conditions. *IEEE Transactions on Industrial Informatics* 2017; 13 (5): 2406-2416. doi: 10.1109/TII.2017.2700327
- [34] Phan BC, Lai YC, Lin CE. A deep reinforcement learning-based MPPT control for PV systems under partial shading condition. *Sensors* 2020; 20 (11): 3039. doi: 10.3390/s20113039
- [35] Avila L, De Paula M, Carlucho I, Reinoso CS. MPPT for PV systems using deep reinforcement learning algorithms. *IEEE Latin America Transactions* 2019; 17 (12): 2020-2027. doi: 10.1109/TLA.2019.9011547
- [36] Tina GM, Ventura C, Ferlito S, De Vito S. A state-of-art-review on machine-learning based methods for PV. *Applied Sciences* 2021; 11 (16): 7550. doi: 10.3390/app11167550

- [37] Xie Z, Wu Z. Maximum power point tracking algorithm of PV system based on irradiance estimation and multi-Kernel extreme learning machine. *Sustainable Energy Technologies and Assessments* 2021; 44: 101090. doi: 10.1016/j.seta.2021.101090
- [38] Padmavathi N, Chilambuchelvan A, Shanker NR. Maximum power point tracking during partial shading effect in pv system using machine learning regression controller. *Journal of Electrical Engineering & Technology* 2021; 16 (2): 737-748. doi: 10.1007/s42835-020-00621-4
- [39] Khan NM, Khan UA, Zafar MH. Maximum Power Point Tracking of PV System under Uniform Irradiance and Partial Shading Conditions using Machine Learning Algorithm Trained by Sailfish Optimizer. In: 2021 4th International Conference on Energy Conservation and Efficiency (ICECE); Lahore, Pakistan; 2021. pp. 1-6. doi: 10.1109/ICECE51984.2021.9406288
- [40] Sarvi M, Azadian A. A comprehensive review and classified comparison of mppt algorithms in pv systems. *Energy Systems* 2021: 1-40.
- [41] Rizzo SA, Scelba G. A hybrid global MPPT searching method for fast variable shading conditions. *Journal of Cleaner Production* 2021; 298: 126775. doi: 10.1016/j.jclepro.2021.126775
- [42] Díaz MD, Trujillo CR, Giral R, Vázquez SL. Evaluation of particle swarm optimization techniques applied to maximum power point tracking in photovoltaic systems. *International Journal of Circuit Theory and Applications* 2021 ; 49 (7): 1849-1867. doi: 10.1002/cta.2978
- [43] Bollipo RB, Mikkili S, Bonthagorla PK. Hybrid, optimal, intelligent and classical PV MPPT techniques: A review. *CSEE Journal of Power and Energy Systems* 2020; 7 (1): 9-33. doi:10.17775/CSEEJPES.2019.02720
- [44] Khan ZA, Khan L, Ahmad S, Mumtaz S, Jafar M et al. RBF neural network based backstepping terminal sliding mode MPPT control technique for PV system. *Plos one* 2021; 16 (4): e0249705. doi: 10.1371/journal.pone.0249705
- [45] Başıoğlu ME, Kazdaloğlu A, Erfidan T, Bilgin MZ, Çakır B. Performance analyzes of different photovoltaic module technologies under İzmit, Kocaeli climatic conditions. *Renewable and Sustainable Energy Reviews* 2015; 52: 357-365. doi: 10.1016/j.rser.2015.07.108
- [46] Minar MR, Naher J. Recent advances in deep learning: An overview. arXiv preprint arXiv:1807.08169, 2018,21.
- [47] Schmidhuber J. Deep learning. 28; 10 (11): 32832: Scholarpedia, 2015.
- [48] Heaton J. Ian goodfellow, yoshua bengio, and aaron courville: Deep learning. Springer, 2018.
- [49] LeCun Y, Bengio Y, Hinton G. Deep learning. *nature* 2015; 521 (7553): 436-444.
- [50] Haykin S. A comprehensive foundation on neural networks. Prentice Hall Upper Saddle River, 1999
- [51] Werbos PJ. Backpropagation through time: what it does and how to do it. In: Proceedings of the IEEE 1990; 78 (10): 1550-1560.
- [52] Hochreiter S, Schmidhuber J. Long short-term memory. *Neural computation* 1997; 9 (8): 1735-1780.
- [53] Gers FA, Schmidhuber J, Cummins F. Learning to forget: Continual prediction with LSTM. *Neural computation* 2000; 12 (10): 2451-2471.
- [54] Lipton ZC, Berkowitz J, Elkan C. A critical review of recurrent neural networks for sequence learning. arXiv preprint arXiv:1506.00019, 2015, 29.
- [55] Kim TY, Cho SB. Predicting residential energy consumption using CNN-LSTM neural networks. *Energy* 2019; 182: 72-81.
- [56] Kong W, Dong ZY, Jia Y, Hill DJ, Xu Y et al. Short-term residential load forecasting based on LSTM recurrent neural network. *IEEE Transactions on Smart Grid* 2017; 10 (1): 841-51.
- [57] Sagheer A, Kotb M. Time series forecasting of petroleum production using deep LSTM recurrent networks. *Neuro-computing* 2019; 323: 203-13.

- [58] Wang JQ, Du Y, Wang J. LSTM based long-term energy consumption prediction with periodicity. *Energy* 2020; 197: 117197.
- [59] Abdel-Nasser M, Mahmoud K. Accurate photovoltaic power forecasting models using deep LSTM-RNN. *Neural Computing and Applications* 2019; 31 (7): 2727-40.